Open access • Journal Article • DOI:10.1049/IET-RPG.2008.0064

Coordinated voltage support in distribution networks with distributed generation and microgrids — Source link

André Madureira, J.A. Pec¸as Lopes

Published on: 29 Sep 2009 - Iet Renewable Power Generation (IET)

Topics: Microgrid, Microgeneration and Distributed generation

Published in IET Renewable Power Generation
Received on 14th July 2008
Revised on 19th December 2008
doi: 10.1049/iet-rpg.2008.0064

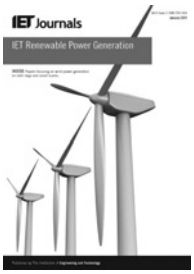

ISSN 1752-1416

Coordinated voltage support in distribution networks with distributed generation and microgrids

A.G. Madureira J.A.Peças Lopes

Power Systems Unit of INESC Porto and Faculty of Engineering of Porto University, Rua Dr. Roberto Frias, 378, Porto 4200-465, Portugal
E-mail: agm@inescporto.pt

Abstract: This paper proposes a new methodology for coordinated voltage support in distribution networks with large integration of distributed generation and microgrids. Given the characteristics of the LV networks, it is shown that traditional control strategies using only reactive power control may not be sufficient in order to perform efficient voltage control. Therefore, microgeneration shedding must also be employed, especially in scenarios with extreme microgeneration penetration. An optimisation tool based on a meta-heuristic approach was developed to address the voltage control problem. In addition, neural networks were employed in order to decrease computational time, thus enabling the use of the tool for online operation. The results obtained revealed good performance of this control approach.

1 Introduction

Electrical distribution networks have been undergoing significant changes in the last few years due to the growth of distributed generation (DG). Nowadays, due to the restructuring process in electrical distribution systems and the implementation of market structures in several European countries, new business opportunities are arising for DG units. Particularly, the connection of these units to the electric power system brings additional control possibilities to the distribution system operator (DSO), and new technical developments enable DG participation in providing ancillary services such as reserves and voltage support [1].

Usually, DG units are not subject to centralis dispatch and reactive power generation is in most cases restricted by the DSO. Therefore, several changes are required in order to fully profit from the benefits resulting from DG integration, and voltage support emerges as one of the main services to be provided by DG units. This results from the fact that a significant growth of DG penetration will require new operation philosophies in order to exploit reactive power generation capability of DG units, with the objective of optimising network operation, minimising active power losses and maintaining voltage profiles.

Several authors have developed interesting work concerning the impact of DG on voltage control in distribution grids [2–5]. In [6], the authors formulate an algorithm for voltage control in distribution grids with DG by solving an optimisation problem, where active power losses are minimised, subject to a set of technical constraints. The control variables to consider are DG reactive power generation, On-line tap changing (OLTC) transformer settings and capacitor bank settings.

One issue that frequently results from high DG penetration is voltage rise problems, especially in weak distribution networks [3, 7]. To overcome this problem, it is necessary to control both active and reactive power of the DG units and/or reduce the voltage at the HV/MV substation [3].

This voltage rise effect is partly the result of DSO policies based on a 'fit and forget' approach, which also requires DG to operate at a fixed power factor, thus limiting the

integration of DG and failing to take full profit of DG ability to mitigate such effects [2, 8].

In addition, it is expected that a similar phenomenon will take place at the low voltage (LV) side of the distribution system, where microgeneration growth will develop rapidly. The connection of microgeneration to LV networks, creating microgrids, will be playing an important role in future distribution networks. The effects seen at the medium voltage (MV) level may propagate to the LV side with even worse consequences, given the high microgeneration penetration.

To overcome the problems resulting from high DG and microgeneration penetration, an effective control scheme must be developed. Formerly, in conventional systems, voltage control was usually considered as a decentralised control problem. This has mainly to do with the fact that voltage is predominantly a local or regional problem.

However, considering this new operation scenario, a decentralised yet hierarchical voltage control scheme must be envisaged, exploiting communication and control possibilities available for microgrid operation [9].

This paper describes a new tool to be used at the distribution management system (DMS) level in order to manage, in an integrated way, voltage control in MV/LV distribution grids in scenarios characterised by large-scale integration of DG, connected at the MV level, and microgeneration, connected at the LV level.

2 Multi-microgrid system architecture

A microgrid comprises an LV feeder with several microsources, storage devices and controllable loads connected on the same feeder [10]. These LV microgrids may be operated in interconnected or in islanded mode (under emergency conditions) and are managed by a microgrid central controller (MGCC) that includes several key functions such as economic management and control functionalities [10, 11].

The new concept of a multi-microgrid is related to a multi-level structure, existing at the MV distribution level, consisting of LV microgrids and DG units connected on adjacent MV feeders. This concept has been developed within the framework of European project More MicroGrids [12]. Therefore, microgrids, DG units and MV loads under demand side management control can be considered in this network as active cells, for control and management purposes. The technical operation of such a system requires the transposition of the microgrid concept to the MV level, where all these active cells should be controlled by a central autonomous management controller (CAMC) to be installed at the MV bus level of an HV/MV substation. The CAMC will serve as an interface to the DMS and operate under the responsibility of the DSO [9].

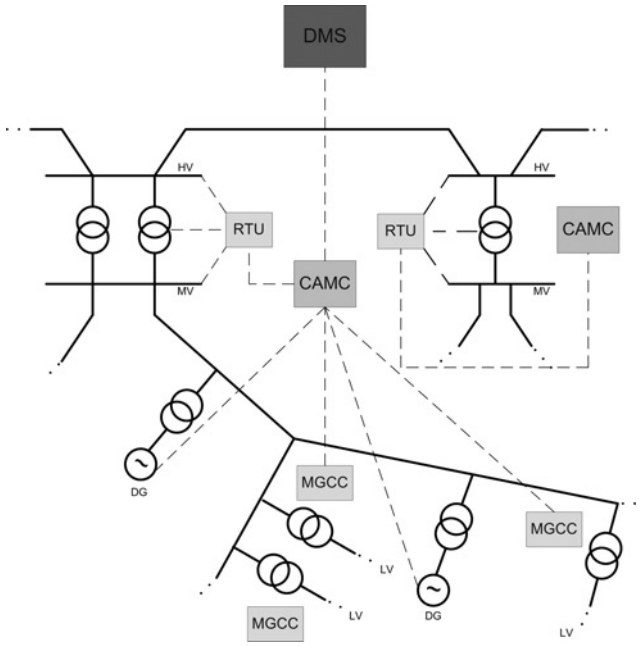

Figure 1 *Control and management architecture of a multi-microgrid system*

This architecture can be seen in Fig. 1.

Nowadays, the DMS is responsible for the supervision, control and management of the distribution system. In future power systems, in addition to the DMS, there will be new management levels:

- The CAMC, to be housed in HV/MV substations, which will accommodate functionalities that are normally assigned to the DMS (or other new functionalities) and will be responsible for interfacing the DMS with lower level controllers.

- The MGCC, to be housed in MV/LV substations, which will be responsible for managing the microgrid, including the control of the microsources and responsive loads. Voltage monitoring in each LV grid will be performed using the microgrid communication infrastructure.

Microgrids, together with DG units, will have a significant impact on the electrical distribution system and will enable the participation of these units in providing ancillary services, such as coordinated voltage support.

3 Voltage control in multi-microgrids

A hierarchical control system must then be established for voltage control in distribution systems comprising large DG and microgeneration penetration, using communication and control possibilities that will become available in future distribution networks.

The main objective of this voltage control system is to ensure an optimised and coordinated strategy between the

doi: 10.1049/iet-rpg.2008.0064

several voltage levels in the distribution system, namely MV and LV.

As previously mentioned, in extreme situations where there is significant voltage rise due to massive DG and microgeneration penetration, reactive power control is not sufficient to maintain efficient system operation, especially in LV networks where the X/R index is low. Consider the example system presented in Fig. 2.

Given the example system presented and considering that, in LV networks, the line resistance is greater than the line reactance (i.e. $R > X$), the following expression may be derived from the power flow equations:

$$P_{\text{inj}} = \frac{V_2^2}{R} - \frac{V_2 V_1}{R}\cos(\delta) \tag{1}$$

where P_{inj} is the active power injected in the MV network, V_2 is the bus voltage at the LV network (microgrid), V_1 is the bus voltage at the MV network, R is the branch resistance and δ is the angle between V_1 and V_2.

According to (1), it may be seen that in order to be able to inject active power (P_{inj}) from the LV side (microgrid) to the MV side in resistive networks, voltage should be higher at the LV bus (i.e. $V_2 > V_1$).

It must be stressed that the low X/R ratio applies only to branches in the LV microgrid since, in this work, transformers in grid-connected mode are not modelled in the LV microgrid.

Therefore, high DG and microgeneration penetration will require the development of an effective voltage control scheme based on active and reactive power control since the decoupling between active power and voltage is not valid in LV networks. In the case of LV grids with microgeneration, the possibility of controlling active power injected by microgeneration units has to be envisaged, since this is the most effective way of controling voltage at the LV level under these conditions.

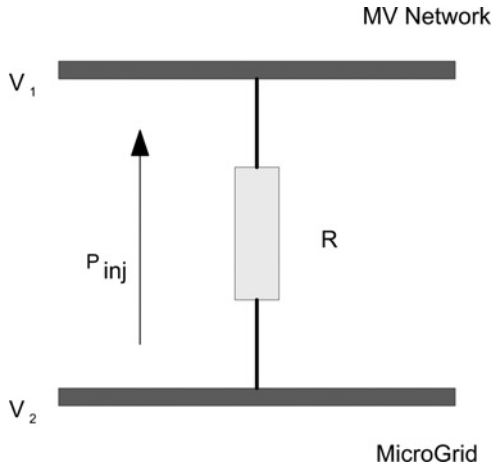

Figure 2 *Example system*

In this paper, a new voltage control procedure is proposed that includes optimising operating conditions by using DG, installed at the MV level, microgrid and OLTC transformer control capabilities. In multi-microgrid systems, it is necessary to address the problem of voltage control at both the MV and the LV levels. To ensure a coordinated operation, a global voltage control algorithm will run at the MV level and the solution obtained will be tested at the LV microgrid level in order to evaluate its feasibility. This approach requires a sequence of global problem solutions and local sub-problem solutions in order to converge to a near-optimum solution.

The voltage control system is designed to be a real-time application that helps the DSO to efficiently manage the distribution network. This proposed functionality comprises a preliminary stage, where several studies are performed offline in order to evaluate the performance of the algorithm given the characteristics of the network and adequately select the parameters for the optimisation problem formulation. Only then, the optimisation tool may be used in real-time operation and made available to the operator.

3.1 Mathematical formulation

The voltage control problem for multi-microgrid systems is a non-linear optimisation problem that can be formulated as shown in (2).

$$\min \text{OF}(\underline{X})$$

subject to

$$\begin{aligned} V_i^{\min} &\le V_i \le V_i^{\max} \\ S_{ik}^{\min} &\le S_{ik} \le S_{ik}^{\max} \\ t_i^{\min} &\le t_i \le t_i^{\max} \\ Q_i^{\min} &\le Q_i \le Q_i^{\max} \end{aligned} \tag{2}$$

where OF is the objective function, X is the control variables, V_i is the voltage at bus i, $V_i^{\min}$, $V_i^{\max}$ are the minimum and maximum voltage at bus i, S_{ik} is the power flow in branch ik, $S_{ik}^{\min}$, $S_{ik}^{\max}$ are the minimum and maximum power flows in branch ik, t_i is the transformer tap of or capacitor step position and$t_i^{\min}$, $t_i^{\max}$ are the minimum and maximum tap.

The objective function chosen aims at minimising active power losses and microgeneration shedding and is shown in (3).

$$\min \quad \sum P_{\text{loss}} + \sum \mu G_{\text{shed}} \tag{3}$$

where P_{loss} is the active power losses andμG_{shed} is the amount of microgeneration shed.

Active power losses were assessed as a function of the line resistance and the current flowing in each line after a power

flow routine. The total active power losses used in the objective function are calculated as the sum of the active power losses in each line.

3.2 Optimisation algorithm

Given the characteristics of the problem under analysis, with a large dimension and a mixed continuous/integer nature concerning the control variables (possibility of controlling active and reactive generation levels – continuous variables, and transformer taps/capacitor banks – integer variables), a meta-heuristic approach was chosen. The optimisation algorithm used in this work was evolutionary particle swarm optimization (EPSO). This algorithm is a combination of traditional particle swarm intelligence, developed by Kennedy and Eberhardt [13], and evolutionary strategies, developed by Schwefel [14], and has been used extensively in optimisation problems for electrical power systems. More details on the algorithm can be found in [15, 16].

The variables or parameters in EPSO are divided into object parameters (the X variables – control parameters of the problem) and strategic parameters (the weights w). The algorithm considers a set of solutions or alternatives that are called particles. The X variables include all the control variables used in the voltage and reactive power control optimisation problem, as described in Section 3.1. Strategic parameters (w) are used to control the behaviour of the optimisation algorithm.

In EPSO, each particle (or solution at a given stage) is defined by its position X_i^k and velocity v_i^k for the coordinate position i and particle k.

The general scheme of EPSO is presented next:

- Replication – each particle is replicated r times.
- Mutation – each particle has its weights w mutated.
- Reproduction – each particle generates an offspring according to the particle movement rule.
- Evaluation – each offspring has its fitness evaluated.
- Selection – the best particles are selected by stochastic tournament.

The particle movement rule is the following: given a particle X_i, a new particle X_i^{new} can be obtained from (4).

$$X_i^{\text{new}} = X_i + v_i^{\text{new}} \tag{4}$$

with

$$v_i^{\text{new}} = w_{i0}^* V_i + w_{i1}^*(b_i - X_i) + w_{i2}^*(b_g^* - X_i) \tag{5}$$

where X_i is the position of the particle, v_i is the velocity of the particle, w_{ik}^* is the strategic parameter (weight), b_i is the best solution of each particle and b_g^* is the best solution among all particles.

The weights (w_{ik}^*) are mutated as shown in (6).

$$w_{ik}^* = w_{ik} + \tau N(0, 1) \tag{6}$$

where τ is the fixed learning parameter and $N(0, 1)$ is the random variable with Gaussian distribution, 0 mean and variance 1.

The global best (b_g^*) is also mutated as shown in (7).

$$b_g^* = b_g + \tau' N(0, 1) \tag{7}$$

where τ' is the fixed learning parameter.

The control variables used in this work were:

- Reactive power from DG sources.
- Active power from microgrids by means of microgeneration shedding (assuming that all microsources are curtailed in the same proportion).
- Reactive power from microgrids by means of capacitor banks located at the MV/LV transformer substation of each microgrid.
- OLTC transformer settings at distribution transformers.

These control variables are used as set-points sent to each device (DG unit, microgrid or OLTC transformer) using the control scheme presented in Fig. 1. For instance, considering the active power of microgeneration, a set-point is sent to the MGCC indicating that microgeneration should be reduced according to that set-point. This information is then sent to individual microsource controllers (as defined in the control structure presented in [10]) that receive an individual set-point in order to lower their generation.

In this work, the constraints were dealt with in traditional evolutionary strategies, that is, using a penalty approach.

3.3 Artificial neural network

As previously mentioned, the voltage control scheme presented is intended to be used as an online function, made available to the DSO. Therefore, and in order to speed up the control algorithm, an artificial neural network (ANN) able to emulate the behaviour of the LV network (or microgrid) was included. This option enables the use of the meta-heuristic tool employed in real-time operation, reducing the long simulation times that were required in order to calculate consecutive LV power flows. In fact, the ANN is used to provide a steady-state equivalent of the microgrid, avoiding in this way the extension of the load flow analysis to the LV microgrid level. Using the ANN, the computational burden and consequently the computational time have significantly decreased.

doi: 10.1049/iet-rpg.2008.0064

The ANN to be employed has the following inputs:

- Voltage at the MV/LV substation.
- Active power generated by each microgenerator unit.
- Total load of the microgrid.

The two outputs are the active power losses and the maximum voltage inside the microgrid, since one of the most critical problems to be addressed is related with overvoltage problems that may occur.

To achieve good performance, different ANN topologies (different number of layers and number of neurons in each hidden layer) were tested. The ANN with the best performance has eight inputs, one hidden layer with 24 neurons and two outputs.

To generate the data set corresponding to the inputs chosen to train the ANN, a large number of power flows were computed, considering different combinations of the inputs (i.e. several values for the voltage reference at the MV/LV substation, for the power generated by each microsource and for the load) in order to calculate the active power losses and assess the voltage profiles in each scenario.

The generated data set contains 11 664 operating points, which were split into a training set and a test set containing 2/3 and 1/3 of the total operating points, respectively. The training set was used for training the ANN and the test set for performance evaluation purposes. The MATLAB Neural Network Toolbox using the Levenberg–Marquart back-propagation algorithm was used to identify the ANN parameters.

The performance obtained can be evaluated in terms of the mean absolute error (MAE). The MAE obtained for one of the outputs (active power losses) was 1.01×10^{-3}. Despite the simple structure adopted for the ANN, the performance parameters illustrated the quality of the tool for emulating the behaviour of the microgrid.

Nevertheless, in case of microgrid reconfiguration (due to adding of a new microgenerator, for instance), a new ANN must be computed. This means that it is necessary to update the data for the power flow and then generate a new data set and train a new ANN that emulates the LV microgrid steady-state behaviour.

4 Test case networks and scenarios

To test the voltage control approach developed, two real distribution networks were used: an MV distribution network and an LV distribution network shown in Figs. 3 and 4, respectively.

The MV network used is a rural network with two distinct areas with different voltage levels: 30 kV at node NO119 and

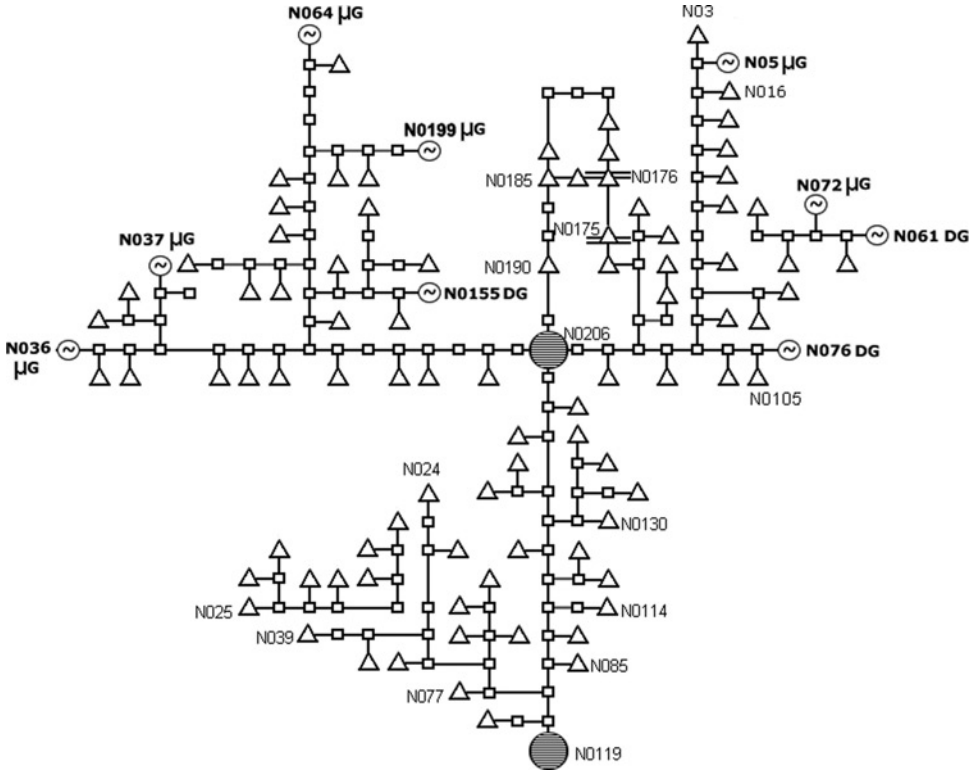

Figure 3 *MV test network*

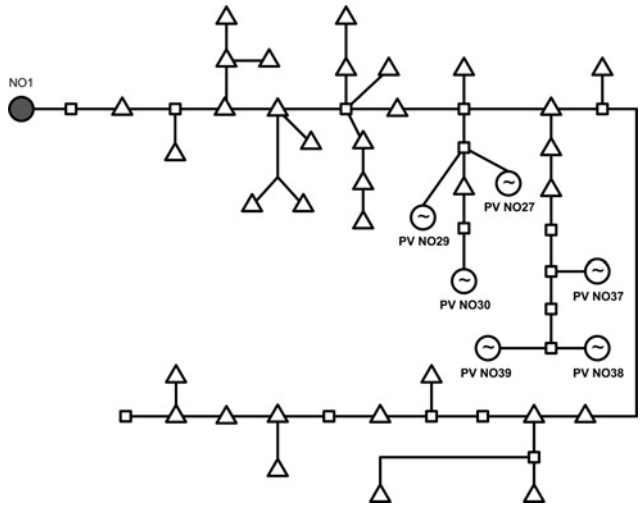

Figure 4 *LV test network*

15 kV after the 30 kV/15 kV transformer at node NO206. It comprises six microgrids (marked as μG in Fig. 3), all with a similar topology, and 3 DG units (marked as DG in Fig. 3) based on Combined Heat and Power – CHP (NO3 in Fig. 3) and wind (NO16 and N061 in Fig. 3).

The LV network (microgrid) used is also a rural network with a radial structure. It was considered that all microgrids have the same structure (shown in Fig. 4). As previously stated, this LV network was used to train the ANN that was included in the optimisation algorithm.

Data on the test networks used in this work are presented in Tables 2–5.

Each microgrid is supposed to comprise six microgenerators, all photovoltaic units (marked as PV in Fig. 4). The ANN is, however, capable of dealing with different levels of microgeneration penetration, as well as with different locations for the microsources.

Table 1 Test case scenarios for generation

Test network	Distributed generation/microgeneration	
	Installed capacity, MW	Percentage peak load, %
MV	3.6	60
LV	0.1	100

In this approach, from the MV point of view, each LV microgrid was considered as a single bus with an equivalent generator (corresponding to the sum of all micro-source generations) and equivalent load (corresponding to the sum of all LV loads).

Typical generation curves for each generating technology (CHP, Wind and PV) were used, as well as typical load curves, for a 24 h period.

The total generation installed capacity for the scenarios used is presented in Table 1.

The 24 h profile of the total load (a mix of residential and commercial consumers) in the MV network is presented in Fig. 5.

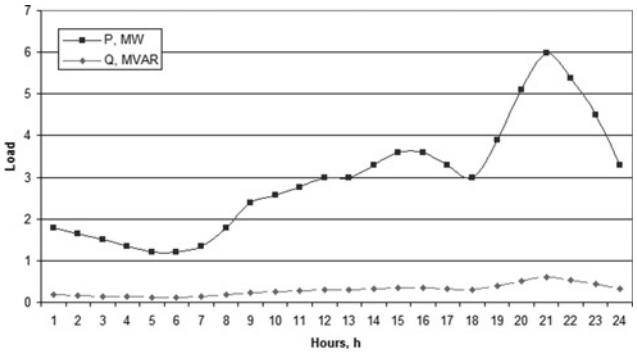

Figure 5 *MV test network total load*

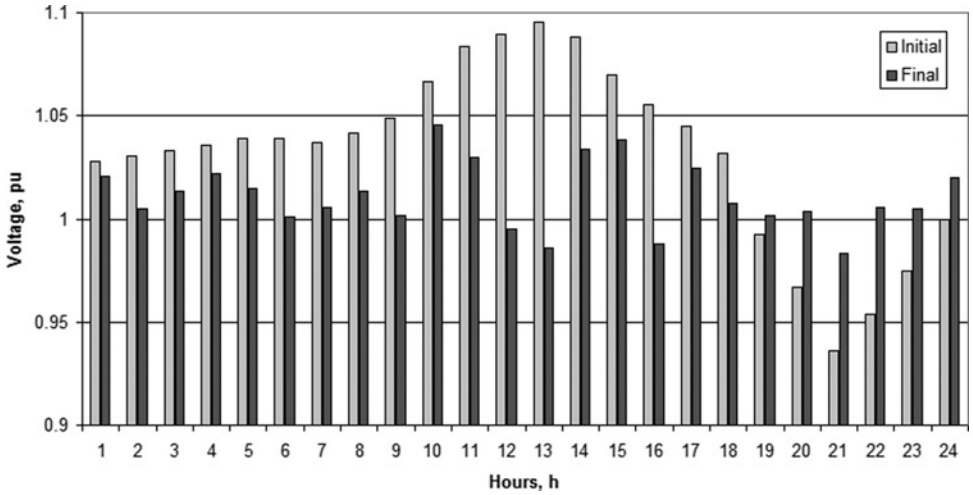

Figure 6 *Maximum voltage values in microgrid at node 64*

doi: 10.1049/iet-rpg.2008.0064

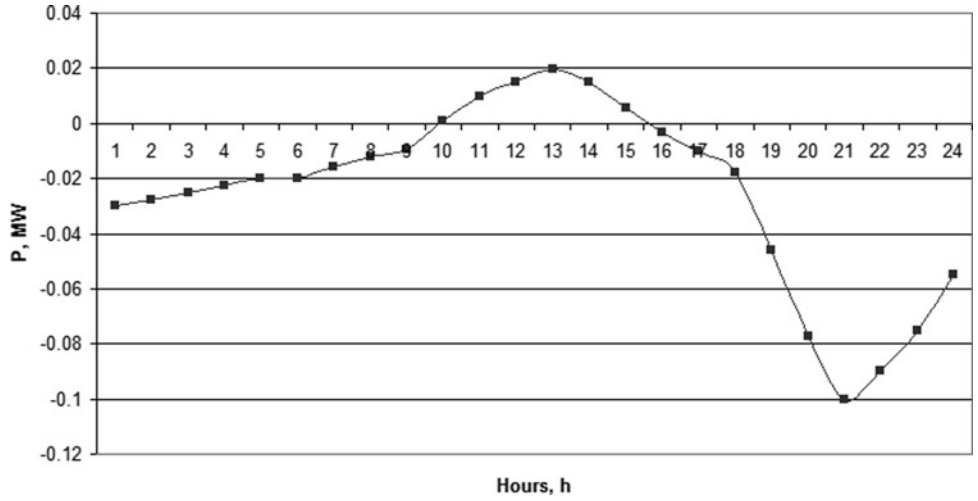

Figure 7 *Active power exported to the MV network by the microgrid at node 64*

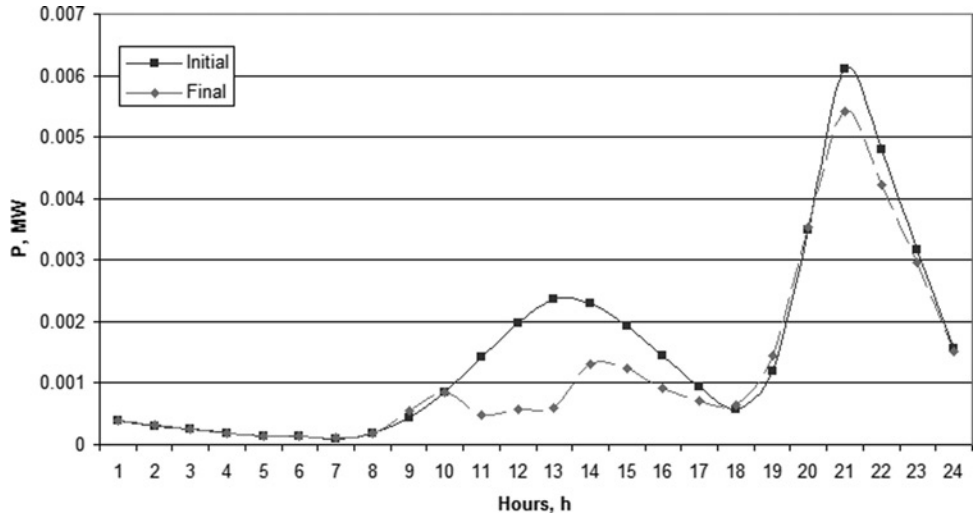

Figure 8 *Active power losses in microgrid at node 64*

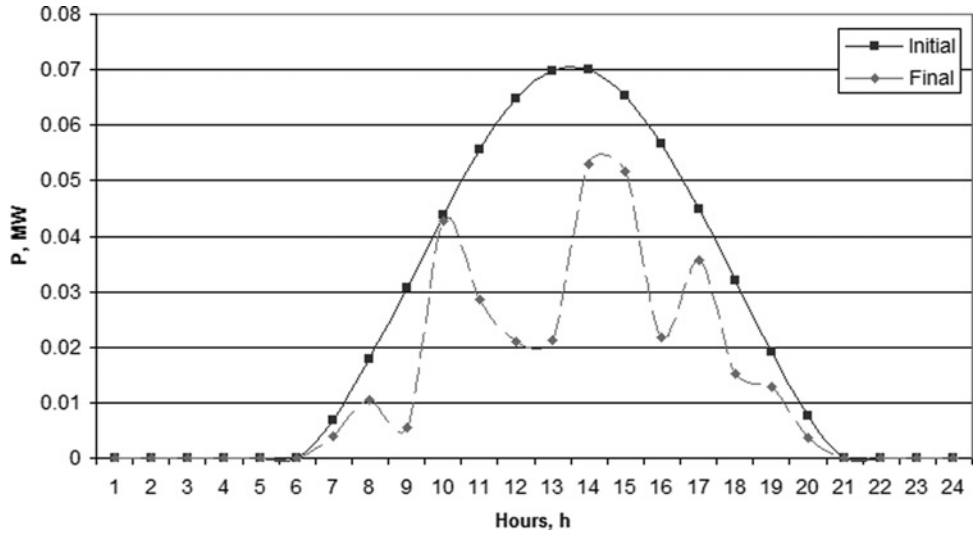

Figure 9 *Total microgeneration in microgrid at node 64*

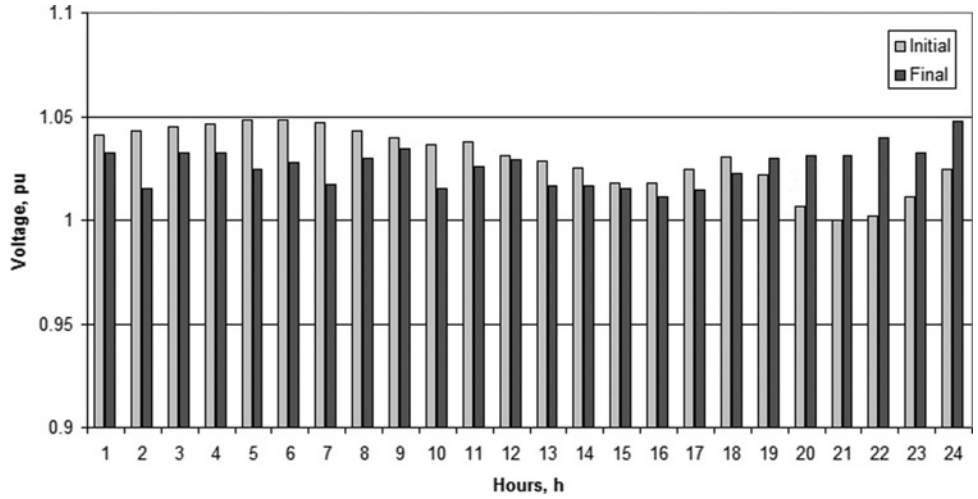

Figure 10 *Maximum voltage values in the MV network*

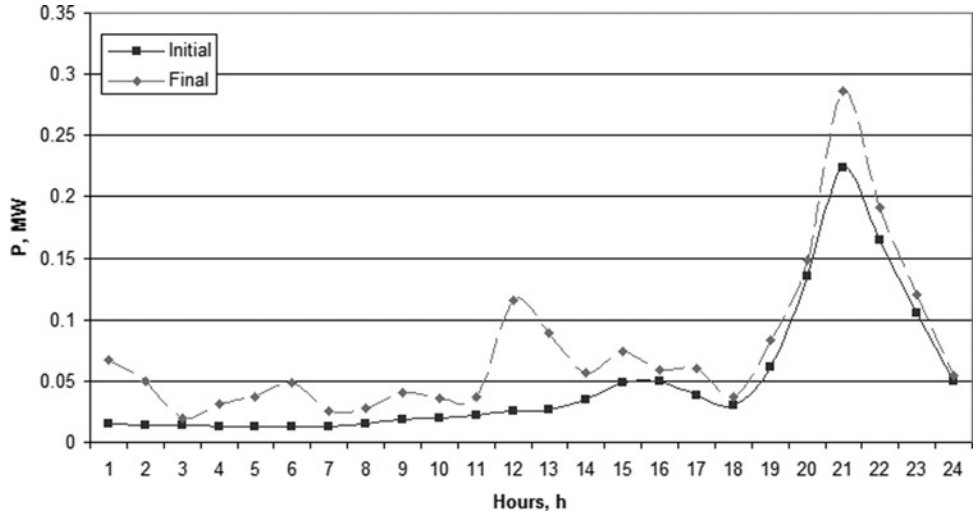

Figure 11 *Active power losses in the MV network*

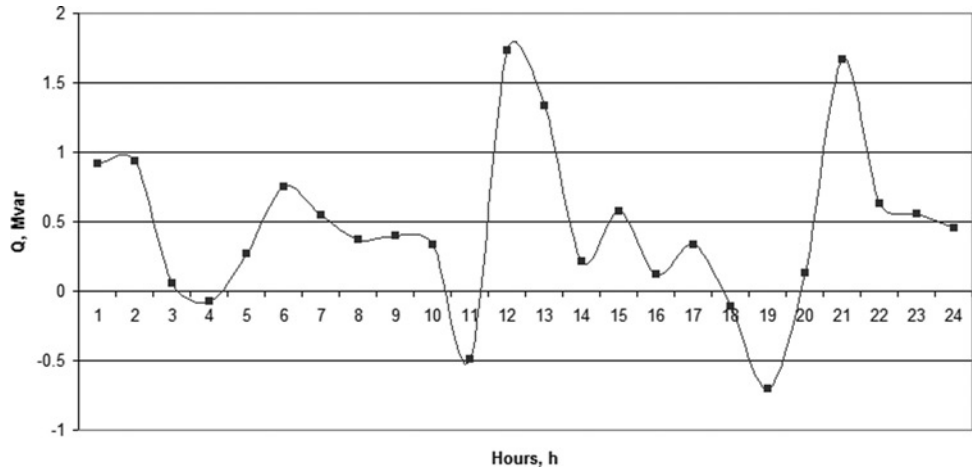

Figure 12 *Total reactive power provided by DG and microgeneration*

doi: 10.1049/iet-rpg.2008.0064

Table 2 LV test network line data

From bus	To bus	Length, m	*R*, ohm/km	*L*, mH/km
NO1	NO2	16	0.164	0.22
NO2	NO3	23	0.32	0.23
NO3	NO4	25	0.443	0.25
NO4	NO5	3	3.08	0.44
NO4	NO6	24	0.443	0.25
NO6	NO7	22	1.2	0.27
NO7	NO8	5	3.08	0.44
NO7	NO9	25	12.6	0.32
NO6	NO10	22	0.443	0.25
NO10	NO11	15	3.08	0.44
NO10	NO12	12	3.08	0.44
NO10	NO13	13	3.08	0.44
NO10	NO14	29	0.443	0.25
NO14	NO15	9	3.08	0.32
NO14	NO16	27	1.2	0.27
NO16	NO17	3	3.08	0.44
NO14	NO18	2	3.08	0.44
NO18	NO19	3	3.08	0.44
NO19	NO20	4	3.08	0.44
NO14	NO21	19	0.443	0.25
NO21	NO22	17	0.443	0.25
NO22	NO23	12	0.868	0.24
NO22	NO24	34	0.443	0.25
NO24	NO25	26	0.868	0.24
NO24	NO26	6	3.08	0.44
NO24	NO27	15	3.08	0.44
NO24	NO28	24	1.2	0.27
NO27	NO29	13	3.08	0.44
NO22	NO30	3	0.443	0.25
NO30	NO31	2	3.08	0.44
NO30	NO32	12	0.443	0.25
NO32	NO33	24	0.443	0.25
NO33	NO34	22	3.08	0.32
NO34	NO35	54	3.08	0.32
NO35	NO36	61	3.08	0.32
NO36	NO37	7	3.08	0.32
NO32	NO38	30	0.443	0.25
NO38	NO39	12	1.2	0.27
NO38	NO40	23	0.443	0.25
NO40	NO41	33	0.443	0.25
NO41	NO42	51	1.2	0.27
NO41	NO43	126	1.2	0.27
NO41	NO44	90	0.443	0.25
NO44	NO45	15	3.08	0.32
NO44	NO46	33	0.443	0.25
NO46	NO47	54	0.443	0.25
NO47	NO48	33	3.08	0.32
NO47	NO49	40	0.443	0.25
NO49	NO50	30	0.443	0.25
NO50	NO51	30	1.2	0.27
NO50	NO52	188	0.641	0.26

5 Results and discussion

This control algorithm was implemented in the MATLAB environment, using MATPOWER [17] to calculate the power flows and MATLAB Neural Network Toolbox to design the ANN.

The objective function for the optimisation problem aimed at reducing active power losses while maintaining voltage profiles within admissible limits ($\pm$5%).

For the optimisation algorithm, a maximum of 100 iterations were used for each hour of the day for a total time horizon of one day. Typical 24 h curves for each generation technology and for the load (considered similar in all load nodes) have been developed for that purpose.

The control variables used are presented in (8).

$$P_{\mu G1}|\ldots|P_{\mu G6}|Q_{\mu G1}|\ldots|Q_{\mu G6}|Q_{DG1}|\ldots|Q_{DG3}|t_{tap} \quad (8)$$

where $P_{\mu Gi}$ is the active power generated by microgrid i, $Q_{\mu Gi}$ is the reactive power generated by microgrid i, Q_{DGi} is the reactive power generated by DG unit i and t_{ltap} is the tap value in the transformer at node 206.

The main results obtained are presented in the following figures.

Table 3 LV test network bus data

Bus no.	Load, kVA
NO3	6.9
NO5	31.05
NO6	6.9
NO7	10.35
NO8	6.9
NO9	10.35
NO10	3.45
NO11	27.6
NO12	6.9
NO13	6.9
NO15	6.9
NO16	10.35
NO17	6.9
NO18	3.45
NO19	3.45
NO20	6.9
NO21	34.5
NO23	13.8
NO25	20.7
NO26	13.8
NO27	6.9
NO28	13.8
NO29	24.15
NO30	10.35
NO31	13.8
NO32	3.45
NO33	17.25
NO34	10.35
NO35	20.7
NO36	3.45
NO37	6.9
NO39	20.7
NO40	10.35
NO41	10.35
NO42	20.7
NO43	41.5
NO45	10.35
NO46	10.35
NO47	10.35
NO48	6.9
NO49	10.35
NO50	10.35
NO51	10.35

Fig. 6 compares the base situation without the voltage control functionality (Initial) and the result obtained after the application of the control algorithm (Final) in the LV microgrid. It can be seen that the voltage values were out of the admissible range of $\pm 5\%$ due to the massive penetration of PV-based microgeneration that generated power outside peak demand hours.

Fig. 7 shows that the microgrid exports power to the upstream network between 10 and 16 h (sunny hours) and imports in the remaining hours, including during peak load at 21 h. Nevertheless, the voltage control functionality succeeded in bringing the voltages back into the admissible range, either during daytime when voltages were too high or during night-time when voltages were low.

In addition, active power losses (Fig. 8) in the microgrid are reduced since some microgeneration shedding (Fig. 9) was required during the sunniest hours in order to bring voltage profiles back within admissible limits. The high losses in the base case (Initial in Fig. 8) are due to the fact that microgeneration penetration was extremely high regarding the local load level and the location of the microgeneration was not ideal.

Concerning the MV network, it may be observed in Fig. 10 that voltage values were inside admissible values, despite the fact that the control algorithm had to raise voltages during night-time in order to be able to also raise voltage within the microgrids (Fig. 6).

Fig. 11 shows that the MV network losses have increased slightly, which is natural given that the main concern in this network was poor voltage profiles.

Fig. 12 presents the evolution of reactive power generated (positive values) or absorbed (negative values) by the DG sources and the microgrids in order to aid voltage control. The base case (Initial) is not shown since it considered a unity power factor for all generating sources.

doi: 10.1049/iet-rpg.2008.0064

Table 4 MV test network line data

From bus	To bus	Length, m	*R*, ohm/km	*L*, mH/km
NO206	NO202	68	0.324	0.10
NO200	NO206	666	0.521	0.38
NO206	NO201	71	0.324	0.10
NO206	NO203	50	0.324	0.10
NO118	NO119	842	0.521	0.38
NO176	NO174	490	0.324	0.10
NO175	NO176	90	0.324	0.10
NO176	NO182	262	0.627	0.11
NO131	NO133	27	0.731	0.39
NO132	NO122	756	0.731	0.39
NO29	NO30	323	0.731	0.39
NO62	NO58	604	0.731	0.39
NO79	NO77	46	0.731	0.39
NO57	NO56	481	1.181	0.40
NO189	NO192	100	1.608	0.41
NO184	NO182	236	0.324	0.10
NO44	NO45	661	1.181	0.40
NO111	NO104	474	0.324	0.12
NO134	NO135	119	1.181	0.40
NO201	NO190	1349	0.731	0.39
NO190	NO187	183	0.463	0.10
NO162	NO163	105	0.731	0.39
NO194	NO208	1364	1.643	0.41
NO110	NO114	2	0.561	0.40
NO175	NO171	210	0.627	0.11
NO168	NO171	325	1.608	0.41
NO185	NO191	250	0.568	0.11
NO193	NO191	54	0.463	0.10
NO75	NO74	217	0.731	0.39
NO183	NO178	64	1.181	0.40
NO147	NO149	20	0.733	0.41
NO138	NO139	35	0.568	0.11
NO90	NO86	163	0.731	0.39
NO23	NO24	539	1.608	0.41
NO65	NO73	528	1.181	0.40

Continued

Table 4 *Continued*

From bus	To bus	Length, m	*R*, ohm/km	*L*, mH/km
NO112	NO105	406	1.608	0.41
NO48	NO51	758	0.731	0.39
NO97	NO80	1066	0.731	0.39
NO44	NO34	634	0.731	0.39
NO88	NO89	13	0.731	0.39
NO88	NO64	1552	0.731	0.39
NO31	NO36	1177	0.731	0.39
NO106	NO92	1058	1.181	0.40
NO78	NO63	1404	1.608	0.41
NO204	NO209	613	0.731	0.39
NO204	NO205	41	0.731	0.39
NO14	NO13	10	1.181	0.40
NO156	NO158	1310	0.731	0.39
NO15	NO16	21	0.731	0.39
NO38	NO37	199	1.643	0.41
NO68	NO66	669	0.731	0.39
NO68	NO61	555	0.731	0.39
NO107	NO109	10	1.181	0.40
NO196	NO199	480	0.568	0.11
NO120	NO121	9	1.608	0.41
NO127	NO130	172	1.181	0.40
NO40	NO42	12	0.731	0.39
NO46	NO49	696	0.731	0.39
NO161	NO180	812	1.181	0.40
NO161	NO160	10	1.181	0.40
NO151	NO150	64	0.568	0.13
NO69	NO60	1227	0.731	0.39
NO166	NO169	38	1.181	0.40
NO55	NO53	1217	0.731	0.39
NO75	NO81	399	0.731	0.39
NO129	NO128	275	1.181	0.40
NO167	NO170	56	1.181	0.40
NO185	NO174	536	0.532	0.11
NO90	NO96	682	0.731	0.39
NO31	NO28	594	0.731	0.39

Continued

Table 4 *Continued*

From bus	To bus	Length, m	*R*, ohm/km	*L*, mH/km
NO100	NO101	11	1.181	0.40
NO100	NO84	1006	0.731	0.39
NO94	NO85	711	0.731	0.39
NO12	NO4	2234	0.731	0.39
NO12	NO2	1561	0.731	0.39
NO10	NO17	638	0.731	0.39
NO162	NO144	1073	1.608	0.41
NO103	NO91	649	1.608	0.41
NO8	NO7	42	1.181	0.40
NO11	NO9	681	0.731	0.39
NO153	NO164	699	0.731	0.39
NO153	NO155	245	1.181	0.40
NO112	NO76	2286	1.608	0.41
NO83	NO82	1833	0.731	0.39
NO148	NO141	343	1.181	0.40
NO140	NO154	821	1.181	0.40
NO198	NO207	1218	0.731	0.39
NO173	NO172	136	1.181	0.40
NO41	NO39	176	1.608	0.41
NO18	NO19	924	0.731	0.39
NO8	NO1	2520	0.731	0.39
NO26	NO25	3	0.324	0.12
NO126	NO123	167	0.731	0.39
NO32	NO33	257	0.731	0.39
NO157	NO167	703	0.731	0.39
NO197	NO195	10	0.731	0.39
NO6	NO5	394	1.181	0.40
NO52	NO54	272	1.181	0.40
NO3	NO6	436	0.731	0.39
NO69	NO71	82	0.731	0.39
NO181	NO184	154	0.324	0.10
NO186	NO185	94	0.463	0.10
NO145	NO143	63	1.181	0.40
NO22	NO20	407	0.919	0.39
NO125	NO124	30	1.181	0.40

Continued

Table 4 *Continued*

From bus	To bus	Length, m	*R*, ohm/km	*L*, mH/km
NO6	NO15	1188	0.411	0.38
NO10	NO8	515	1.181	0.40
NO11	NO10	302	1.181	0.40
NO18	NO11	1114	1.181	0.40
NO14	NO12	330	0.731	0.39
NO21	NO14	977	0.731	0.39
NO15	NO29	2412	0.411	0.38
NO21	NO18	594	1.181	0.40
NO27	NO21	1114	1.181	0.40
NO27	NO22	1394	0.919	0.39
NO22	NO23	610	1.608	0.41
NO41	NO26	2688	0.731	0.39
NO29	NO32	518	0.411	0.38
NO48	NO31	3460	0.731	0.39
NO32	NO42	952	0.411	0.38
NO38	NO35	138	0.731	0.39
NO43	NO38	320	0.731	0.39
NO43	NO44	735	1.181	0.40
NO50	NO43	1536	0.731	0.39
NO47	NO27	3422	0.919	0.39
NO47	NO41	1460	1.608	0.41
NO55	NO47	2024	0.919	0.39
NO50	NO48	1798	0.731	0.39
NO52	NO50	204	0.731	0.39
NO57	NO52	879	0.731	0.39
NO70	NO55	1589	0.919	0.39
NO78	NO57	1476	0.731	0.39
NO49	NO59	2060	0.411	0.38
NO59	NO83	1449	0.411	0.38
NO59	NO62	454	0.731	0.39
NO62	NO65	550	0.731	0.39
NO65	NO67	379	0.731	0.39
NO67	NO68	175	0.731	0.39
NO75	NO69	847	0.731	0.39
NO79	NO70	605	0.919	0.39

Continued

IET Renew. Power Gener., 2009, Vol. 3, Iss. 4, pp. 439–454
doi: 10.1049/iet-rpg.2008.0064

Table 4 *Continued*

From bus	To bus	Length, m	*R*, ohm/km	*L*, mH/km
NO70	NO75	466	0.731	0.39
NO99	NO78	1380	0.731	0.39
NO93	NO79	1377	0.919	0.39
NO83	NO87	536	0.411	0.38
NO87	NO90	395	0.731	0.39
NO87	NO131	3561	0.411	0.38
NO93	NO94	1177	0.521	0.38
NO118	NO93	5019	0.521	0.38
NO94	NO97	1100	0.521	0.38
NO97	NO98	60	0.521	0.38
NO98	NO110	872	0.919	0.39
NO98	NO102	2643	0.521	0.38
NO99	NO103	1494	0.731	0.39
NO106	NO99	712	0.731	0.39
NO102	NO100	102	0.731	0.39
NO102	NO107	839	0.521	0.38
NO103	NO108	954	0.731	0.39
NO115	NO106	935	0.731	0.39
NO107	NO117	1521	0.521	0.38
NO108	NO134	1714	1.608	0.41
NO108	NO116	2589	0.731	0.39
NO118	NO111	738	0.919	0.39
NO132	NO112	1891	1.608	0.41
NO125	NO115	1261	0.731	0.39
NO116	NO140	1559	1.181	0.40
NO116	NO120	1698	0.731	0.39
NO117	NO165	5165	0.521	0.38
NO117	NO127	745	1.181	0.40
NO120	NO126	913	0.731	0.39
NO166	NO125	2295	0.731	0.39
NO126	NO129	457	1.608	0.41
NO127	NO152	1511	1.181	0.40
NO129	NO136	268	1.608	0.41
NO131	NO137	669	0.411	0.38
NO137	NO132	517	1.608	0.41

Continued

Table 4 *Continued*

From bus	To bus	Length, m	*R*, ohm/km	*L*, mH/km
NO134	NO142	494	1.608	0.41
NO136	NO156	1363	1.608	0.41
NO136	NO113	3080	0.731	0.39
NO173	NO137	3436	0.411	0.38
NO146	NO138	634	0.731	0.39
NO140	NO148	405	1.181	0.40
NO142	NO153	1009	0.731	0.39
NO142	NO146	180	1.608	0.41
NO148	NO145	61	1.181	0.40
NO146	NO147	68	1.608	0.41
NO152	NO151	231	1.181	0.40
NO152	NO161	536	1.181	0.40
NO156	NO189	1611	1.608	0.41
NO179	NO159	1117	0.731	0.39
NO159	NO168	364	1.608	0.41
NO159	NO162	161	0.731	0.39
NO165	NO204	2069	0.731	0.39
NO165	NO197	2090	0.521	0.38
NO177	NO166	453	0.731	0.39
NO168	NO167	516	1.181	0.40
NO179	NO173	364	0.411	0.38
NO183	NO177	195	0.731	0.39
NO194	NO179	625	0.411	0.38
NO203	NO183	1872	0.731	0.39
NO187	NO186	13	0.532	0.11
NO189	NO196	548	1.181	0.40
NO188	NO193	482	0.870	0.11
NO202	NO194	1144	0.411	0.38
NO197	NO198	97	0.521	0.38
NO198	NO200	817	0.521	0.38
NO113	NO95	988	0.731	0.39
NO95	NO88	387	0.731	0.39
NO42	NO49	2311	0.411	0.38
NO181	NO188	152	1.376	0.12
NO67	NO72	243	0.731	0.39

Table 5 MV test network bus data

Bus no.	Load, kVA
NO176	630
NO133	100
NO122	50
NO30	100
NO58	100
NO77	50
NO56	250
NO192	100
NO182	125
NO45	25
NO104	0
NO135	50
NO190	630
NO163	100
NO208	30
NO114	1335
NO171	100
NO191	630
NO74	160
NO178	50
NO149	500
NO139	1000
NO86	25
NO24	100
NO73	100
NO105	100
NO51	160
NO80	100
NO34	100
NO89	100
NO64	50
NO36	100
NO92	250
NO63	160
NO209	100

Continued

Table 5 *Continued*

Bus no.	Load, kVA
NO205	250
NO13	100
NO158	100
NO16	100
NO37	15
NO66	200
NO61	160
NO109	100
NO199	160
NO121	100
NO130	100
NO40	50
NO46	100
NO180	100
NO160	100
NO150	630
NO60	100
NO169	50
NO175	160
NO53	160
NO81	250
NO128	100
NO170	200
NO174	400
NO96	75
NO28	50
NO101	50
NO84	50
NO85	100
NO4	100
NO2	100
NO17	50
NO144	100
NO91	100
NO7	100

Continued

doi: 10.1049/iet-rpg.2008.0064

Table 5 *Continued*

Bus no.	Load, kVA
NO9	100
NO164	100
NO155	0
NO76	100
NO82	100
NO141	50
NO154	100
NO207	100
NO172	100
NO39	25
NO19	100
NO1	100
NO25	630
NO123	160
NO33	100
NO157	100
NO195	25
NO5	160
NO54	250
NO3	160
NO71	160
NO184	400
NO185	250
NO143	500
NO20	1200
NO124	100
NO72	50

6 Conclusion

Voltage/VAR control in distribution systems integrating microgrids can be treated as a hierarchical optimisation problem that must be analysed in a coordinated way between LV and MV levels.

Given the characteristics of the LV networks, both active and reactive power control is needed for an efficient voltage control scheme.

An optimisation algorithm based on a meta-heuristic was adopted in order to deal with the voltage/VAR control problem at the MV level. The algorithm has proved to be efficient in achieving the main objective function – voltage profile control and active power losses reduction.

The ANN used to emulate the behaviour of the LV microgrid proved to have good performance, enabling reduction of the computational time considerably. The combination of the meta-heuristic optimisation motor together with an ANN equivalent representation of the microgrid allows the use of this approach for real time under DMS environments.

7 Acknowledgments

This work was supported in part by the European Commission within the framework of the More MicroGrids project, Contract no. 019864 – (SES6). The authors would like to thank the research team of the More MicroGrids project for valuable discussions and feedback.

A. G. Madureira wants to express his gratitude to Fundação para a Ciência e a Tecnologia (FCT), Portugal, for supporting this work under grant SFRH/BD/29459/2006.

8 References

[1] JOÓS G., OOI B.T., MCGILLIS D., GALIANA F.D., MARCEAU R.: 'The potential of distributed generation to provide ancillary services'. Proc. IEEE PES Summer Meeting, Seattle, USA, July 2000, pp. 1762–1767

[2] VOVOS P.N., KIPRAKIS A.E., WALLACE A.R., HARRISON G.P.: 'Centralized and distributed voltage control: impact on distributed generation penetration', *IEEE Trans. Power Syst.*, 2007, **1**, (22), pp. 476–483

[3] KULMALA A., REPO S., JÄRVENTAUSTA P.: 'Active voltage level management of distribution networks with distributed generation using on load tap changing transformers'. Proc. IEEE Power Tech., Lausanne, Switzerland, July 2007, pp. 455–460

[4] CALDON C., TURRI R., PRANDONI V., SPELTA S.: 'Control issues in MV distribution systems with large-scale integration of distributed generation'. Proc. Bulk Power System Dynamics and Control – VI, Cortina d'Ampezzo, Italy, August 2004, pp. 583–589

[5] NIKNAM T., RANJBAR A., SHIRANI A.: 'Impact of distributed generation on volt/var control in distribution networks'. Proc. IEEE Power Tech., Bologna, Italy, June 2003, pp. 1–6

[6] PEÇAS LOPES J.A., MENDONÇA A., FONSECA N., SECA L.: 'Voltage and reactive power control provided by DG units'. Proc. CIGRE Symp. Power Systems with Dispersed Generation, Athens, Greece, April 2005, pp. 13–16

[7] JENKINS N., ALLAN R., CROSSLEY P., KIRSCHEN D., STRBAC G.: 'Embedded generation' (IEE Power and Energy Series 31, Inst. Elect. Eng, 2000)

[8] MASTERS C.L.: 'Voltage rise: the big issue when connecting embedded generation to long 11 kV overhead lines', *Power Eng. J.*, 2002, **1**, (16), pp. 5–12

[9] MADUREIRA A.G., PEÇAS LOPES J.A.: 'Voltage and reactive power control in MV networks integrating microGrids'. Proc. Int. Conf. Renewable Energy Power Quality, Seville, Spain, March 2007, ICREPQ Webpage: http://www.icrepq.com/icrepq07/386-madureira.pdf

[10] PEÇAS LOPES J.A., MOREIRA C.L., MADUREIRA A.G.: 'Defining control strategies for microGrids islanded operation', *IEEE Trans. Power Syst.*, 2006, **2**, (21), pp. 916–924

[11] PEÇAS LOPES J.A., MOREIRA C.L., MADUREIRA A.G., *ET AL.*: 'Control strategies for microGrids emergency operation'. Proc. Int. Conf. Future Power Syst., Amsterdam, The Netherlands, November 2005, pp. 1–6

[12] MicroGrids Webpage: http://microgrids.power.ece.ntua.gr/micro/index.php, accessed June 2008

[13] KENNEDY J., EBERHART R.C.: 'Particle swarm optimization'. IEEE Int. Conf. Neural Networks, Perth, Australia, November 1995, pp. 1942–1948

[14] SCHWEFEL H.P.: 'Evolution and optimum seeking' (Wiley, 1995)

[15] MIRANDA V., FONSECA N.: 'EPSO – Evolutionary particle swarm optimization, a new algorithm with applications in power systems'. Proc. IEEE Trans. Distribution Conf. Exhibition, October 2002, pp. 6–10

[16] MIRANDA V., FONSECA N.: 'New evolutionary particle swarm algorithm (EPSO) applied to voltage/VAR control'. Proc. Power Syst. Comput. Conf., Seville, Spain, June 2002, pp. 1–6

[17] MATPOWER Webpage: http://www.pserc.cornell.edu/matpower/, accessed June 2008

doi: 10.1049/iet-rpg.2008.0064